On the suitability of spherical glass-body reflectors in industrial applications

Michael LÖSLER[1,*] (0000-0002-1979-263X), Kira-Lynn KOPITZKE[2] (0009-0008-5567-1641) & Cornelia ESCHELBACH[1] (0000-0003-4959-8712)

[1] Laboratory for Industrial Metrology, Faculty 1: Architecture, Civil Engineering, Geomatics, Frankfurt University of Applied Sciences, DE-60318 Frankfurt am Main, Germany
[*] Corresponding author, Email: michael.loesler@fra-uas.de

[2] Marpe Bau GmbH & Co. KG, Hauptstraße 40, DE-34477 Twistetal-Twiste, Germany

DOI: 10.3217/978-3-99161-070-0-014

Abstract

In the field of industrial metrology, spherically mounted reflectors are often used in laser tracker applications. For high-precision measurements, the reflector consists of a mirrored corner cube centred in a steel ball with a typical radius of 1.5″. This spherical design enables a three-point support of the reflector, realised by a magnetic mount, e.g., a drift-nest. In recent years, several surveying equipment suppliers have been offering affordable spherical glass-body reflectors and related accessories for classic terrestrial applications. This development provides a direct physical connection between different types of instruments, such as levelling instruments, total stations, laser scanners or laser trackers, and represents a unified interinstrumental interface. Ensuring an identical point of reference is a necessary condition for interoperability. For that reason, more than thirty spherical glass-body reflectors of different lots were evaluated in terms of precision and reliability. In order to investigate the suitability of these reflectors for industrial applications, the conformity of reference points, zero-point offsets, ball radii, and sphericity were examined in detail and compared with certified references. In addition, radial and lateral deviations as a function of the angle of incidence were studied.

1 Introduction

Measurements with laser-based instruments like total stations are limited by various external effects such as meteorological conditions or the type of the involved reflectors. The effect of meteorology is often reduced by observing the meteorological conditions, i.e., temperature, pressure, humidity, and – if necessary – carbon dioxide, and by applying the first velocity correction to the measured raw distance (RÜEGER, 1996, p. 74f). Alternatively, the meteorologically dependent change in the air refractive index is compensated by using a two-wavelength electro-optical distance measuring unit (EDM) (e.g. GUILLORY ET AL., 2024).

The impact of the involved reflector depends on the reflector type and the reflector composition. As shown by FAVRE & HENNES (2000), a 360° reflector consisting of several small prisms causes different systematic deviations than a commonly used circular standard reflector made of a single glass-body prism. On the one hand, due to the orientation dependent cyclic deviations of 360° reflectors of several millimetres, this reflector type is not recommended for

high-precision measurements (LACKNER & LIENHART, 2016). On the other hand, a standard reflector made of a single glass-body prism is typically characterized by an individual zero-point offset, a centring error, as well as an incident angle dependent radial and lateral deviation pattern as discussed by RÜEGER (1996, p. 148ff). Despite the significant impact on distance measurements, there is currently no specific standard for reflectors. However, both reflector types have been studied extensively, and the interested reader is referred to (e.g. BAUER & LIENHART, 2023; FAVRE & HENNES, 2000; LACKNER & LIENHART, 2016; WIESER, 2026; XIA ET AL., 2006; to cite but a few).

Laser trackers are often used in high-precision industrial applications. The EDM is derived from the Michelson interferometer, allowing distances to be measured with an uncertainty of a few micrometers. To ensure this precision, spherically mounted reflectors (SMR) are used, consisting of a mirrored corner cube centred in a steel ball with a radius of $\tilde{r} = 19.05\,\text{mm}$. Typically, an SMR is magnetically mounted in a drift-nest, as the spherical design enables a three-point support of the reflector. Thus, an aligned SMR enables rotation around the instrument's line of sight and does not consist of a pitch and roll axis like standard reflectors used in terrestrial applications. Moreover, neither a zero-point offset nor radial and lateral deviations occur because an SMR is a glassless reflector. However, the centring of the cube, the ball radius and the sphericity of the surface affect the measurement. For that purpose, these deviations are in the range of a few submicrometers for a high-precision SMR, also used in this investigation as higher-order reference. In recent years, affordable spherical glass-body reflectors (SGR) and related accessories for classic terrestrial applications have been launched by several surveying equipment suppliers. The universal nature of the spherical design represents a unified interinstrumental interface and provides a direct physical connection between different types of instruments, such as levelling instruments, total stations, laser scanners or laser trackers. It even enables a combination of terrestrial observations with photogrammetric measurements. The necessary condition for interoperability is an identical point of reference. This contribution studies the quality of 1.5″ spherical glass-body reflectors and evaluates the suitability of these reflectors for industrial applications.

After a brief description of the data sets, the conformity criteria are presented, the measurement methods are described, and the obtained results are presented and discussed. Section 2.1 evaluates the zero-point offset as the most important property. The radial and lateral deviations are investigated in Sect. 2.2. Geometric properties of the reflectors such as radius and centring are studied in Sect. 2.3. Section 2.4 focuses on deviations from the spherical form of the reflectors. Finally, Sect. 3 concludes this investigation.

2 Spherical glass-body reflectors

In order to investigate the quality of 1.5″ spherical glass-body reflectors, twelve uncertified reflectors (serial no. 1445, purchased in 2013/14), ten certified reflectors (serial no. 1445.SN, purchased in 2020), and fourteen uncertified reflectors (serial no. 1448, purchased in 2024/25) were evaluated. Hereinafter, these different lots are distinguished by their respective serial numbers. The reflectors are manufactured by Bohnenstingl. The certified reflectors were factory checked using a laser tracker AT901 (Hexagon) with an EDM wavelength of 795 nm. Nominal values of the SGR for the ball radius r, the height of the apex a and the distances

between the surface front and the centre b, respectively, as well as the specified zero-point offset c are summarized in Tab 1 (BOHNENSTINGL, 2022, p. 73; BOHNENSTINGL, 2025, p. 54). Figure 1 depicts spherical glass-body reflectors of the three investigated lots. The blue, red and green drift-nests correspond to 1445, 1445.SN and 1448 type reflectors, respectively. Higher-order references are placed in front of the reflectors to be examined.

Fig. 1: Spherical glass-body reflectors of the investigated lots and higher-order references. Back: An uncertified 1445 reflector is mounted on a blue drift-nest, a certified 1445.SN reflector on a red drift-nest, and an uncertified 1448 reflector on a green drift-nest. Front: The glassless reference SMR is a red-ring reflector and mounted on a black drift-nest, while the reference steel ball is mounted on a silver drift-nest.

To evaluate the suitability of spherical glass-body reflectors for industrial applications, all measurements were performed using Hexagon's laser tracker AT960 together with a 1.5″ SMR. The maximum permissible error (MPE) of an observed position is specified by $15\ \mu\text{m} + \frac{6\ \mu\text{m}}{\text{m}}$. The centring, the sphericity and the ball radius of the 1.5″ SMR are specified by $\leq 3\ \mu\text{m}$, and provides a higher-order reference. To reduce the influence of unrecognized meteorological changes, all measurements were performed at a distance of less than 3 m using the instrument's precise measurement mode.

Table 1: Manufacturer specifications for SGR. For the 1445/1445.SN series, the standard deviation of the zero-point offset is derived from the statement that 90% of the values vary within a range of ± 0.1 mm (BOHNENSTINGL, 2022, p. 73), while the standard deviation of the zero-point offset of the 1448 series is derived from the statement that 100% of the values vary within a range of ± 0.1 mm (BOHNENSTINGL, 2025, p. 54).

Parameter name and abbreviation	**Nominal value**	
	1445/1445.SN	**1448**
Ball diameter $2r$	$38.10\ \text{mm} \pm 0.05\ \text{mm}$	$38.10\ \text{mm} \pm 0.03\ \text{mm}$
Apex height above front surface a	$19.30\ \text{mm} \pm 0.20\ \text{mm}$	$19.30\ \text{mm} \pm 0.20\ \text{mm}$
Surface front to centre distance b	$12.55\ \text{mm} \pm 0.10\ \text{mm}$	$12.55\ \text{mm} \pm 0.10\ \text{mm}$
Zero-point offset of uncertified prims c	$-16.90\ \text{mm} \pm 0.06\ \text{mm}$	$-16.90\ \text{mm} \pm 0.03\ \text{mm}$

2.1 Zero-point offset

The most important property of a glass-body reflector is the zero-point offset, which describes the extra path length of the laser beam in the glass-body. According to RÜEGER (1996, p. 157), the offset of an aligned reflector is defined as

$$c = -n\,a + b \tag{1}$$

and depends on the dimension of the reflector and the ratio between the refractive indices of air n_{A} and glass n_{G} given by

$$n = \frac{n_{\mathrm{G}}}{n_{\mathrm{A}}}. \tag{2}$$

According to the equation of VON SELLMEIER (1871), the shorter the wavelength is, the greater is the refractive index. Thus, the zero-point offset depends on the wavelength. Figure 2 depicts the refractive index of BK7 glass as a function of λ (POLYANSKIY 2024). The blue square and the yellow circle indicate a typical wavelength used by total stations and the AT960, respectively. The difference is about $\Delta c = 150$ µm.

If the dimension of the reflector or the wavelength is unknown, the zero-point offset results from the comparison between the reference distance $\tilde{s}$ and the measured distance s to an SGR, i.e.,

$$c = \tilde{s} - s. \tag{3}$$

Measuring the reference reflector yielded $\tilde{s}$ in this investigation. To account for any differences in the reflector's radii, the reflectors were mounted perpendicular to the instrument's line of sight. Each SGR was measured six times, with the SGR being rotated by approximately 60° about the surface normal after each observed distance. The reference distance was measured twice, i.e., at the beginning and the end of each experiment. This procedure was repeated for all reflectors under investigation.

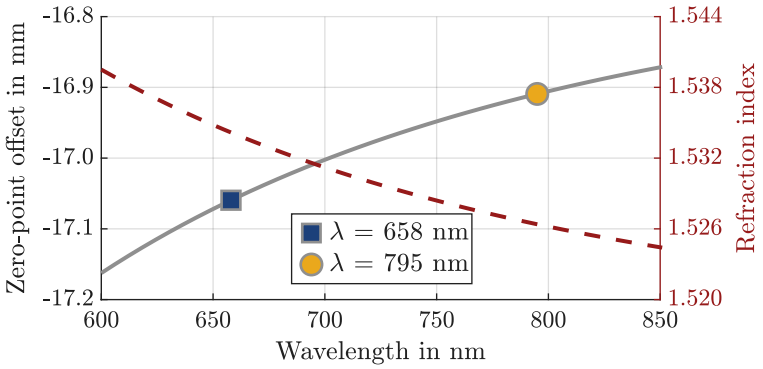

Fig. 2: Zero-point offset $c(\lambda)$ and refractive index $n(\lambda)$ of BK7 glass depicted as solid grey and dashed red curves, respectively, as functions of the wavelength λ. The blue square indicates a typical wavelength used by total stations. The yellow circle relates to the wavelength of the AT960.

Figure 3 shows the derived zero-point offsets of the different lots. The mean standard deviation is about 5 µm for the lots 1445 and 1445.SN, and 8 µm for the lot 1448. However, the zero-point offsets of the reflectors differ significantly, by up to 0.5 mm, and appear to be lot-dependent. The variation of the uncertified 1445 reflectors shown in blue is larger, with differences of up to 0.3 mm occurring.

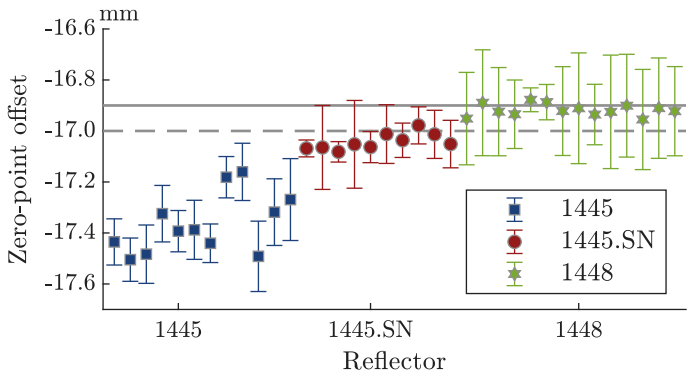

Fig. 3: Derived zero-point offsets. Uncertified 1445 reflectors are represented by blue squares, certified 1445.SN reflectors by red circles, and uncertified 1448 reflectors by green stars. Error bars (1σ) are scaled at a ratio of 20:1. The solid line and the dashed line indicate the nominal value and the certificate value, respectively.

For high-precision measurements, mixing reflectors from different lots is not recommended, even not for total station applications. The mean zero-point offset of the certified 1445.SN reflectors shown in red is about -17.05 mm and varies within a range of less than 0.1 mm. Similar variations are visible for the zero-point offsets of the uncertified 1448 reflectors shown in green. In contrast to the certified reflectors, the mean zero-point offset of the 1448 reflectors is -16.92 mm and closest to the nominal value. Thus, these reflectors are suitable for precise applications. However, the specified zero-point offset should be scrutinised w.r.t. the wavelength of the EDM – even if the reflectors are certified, cf. Fig. 2. Having a total station with an EDM wavelength of 658 nm, the zero-point offset of a certified SGR is about -17.2 mm, and deviates from the nominal value.

2.2 Radial and lateral deviations

Due to the different refractive indices of air and glass, systematic radial and lateral deviations arise, if the reflector is not exactly aligned to the instrument. Using ray tracing, PAULI (1969) derives the radial deviations along the line of sight as a function of the incident angle α, i.e.,

$$\varepsilon_r = a\left(n - \sqrt{n^2 - \sin^2(\alpha)}\right) - b + b\cos(\alpha). \tag{4}$$

As shown by RÜEGER (1978), a misaligned reflector also refracts the beam at the front, resulting in an apparent displacement of the apex. This optical displacement caused lateral deviations perpendicular to the line of sight and can be expressed as

$$\varepsilon_l = (a - b)\sin(\alpha) - a\sec(\alpha_G)\sin(\alpha - \alpha_G), \tag{5}$$

where $\sin(\alpha_G) \coloneqq \frac{1}{n}\sin(\alpha)$ follows from the law of refraction. Both systematic deviations are correctable, whenever the angle of incidence and the dimension of the reflector is sufficiently known (e.g. LÖSLER ET AL., 2013; KOPITZKE 2026).

To study the radial and lateral deviations, an SGM was placed on a rotation stage having the same height as the instrument's inclination axis. A total of six series were measured. In each series, the SGM was rotated from $-45°$ to $45°$ using a step size of $5°$, and each position was observed by the AT960. Afterwards, the SGM was rotated by approximately $60°$ about the surface normal and the procedure was repeated. Figure 4 shows the six series of radial deviations in a range of $\pm 35°$ for the SGR under investigation. The lateral deviations are overlaid by an orientation-dependent pattern. Such a pattern occurs when the necessary orthogonality of the cube sides is not fulfilled and the centre of the prism deviates from the ball centre. This is confirmed by ray tracing on a virtual reflector.

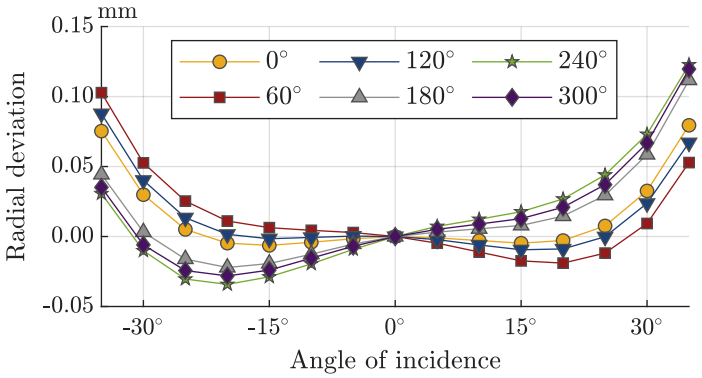

Fig. 4: Lateral deviations w.r.t. the incidence angle and the orientation about the surface normal. To get a better impression of the dependence of the reflector orientation. The incident angle is restricted to $\pm 35°$ to better illustrate the dependence of the deviation on the reflector orientation.

In contrast to standard reflectors consisting of two defined axes of rotation, the orientation about the surface normal of a spherical reflector is arbitrary and almost unpredictable. While a reflector aligning of $\pm 20°$ usually results in negligible deviations as depicted by the yellow series in Fig. 4, large centring deviations lead to additional and unexpected systematic deviations. In order to detect and compare only radial and lateral deviations, the reflectors were carefully pre-aligned.

Figure 5 shows the resulting deviations. The lateral deviations are significantly larger than the radial deviations. The reproducibility of the deviations within a specific lot is quite high, but the results of the lots clearly differ from each other. The uncertified 1445 reflectors yield smallest deviations. Differences in the glass-bodies used between the lots could be one reason for the curve deviations.

Using Eqs. (4), (5), corresponding correction functions were derived by means of a least-squares adjustment, whereby both systematic effects can be compensated for, whenever the angle of incidence is known. Otherwise, a conscientious alignment of the reflectors is strongly recommended for high-precision applications.

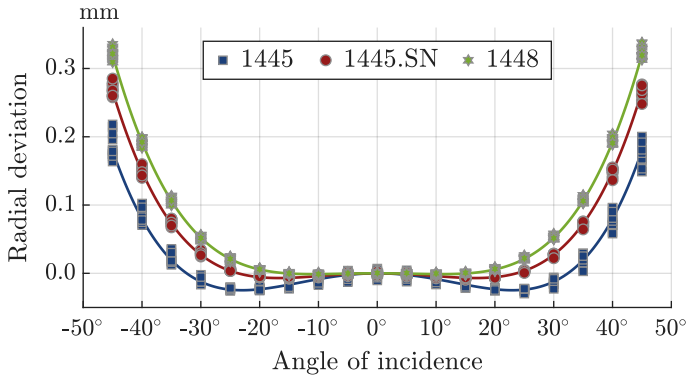

(a) Radial deviations

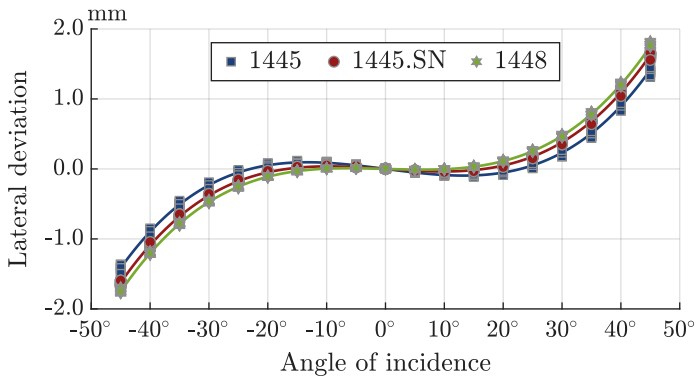

(b) Lateral deviations

Fig. 5: Lateral and radial deviation of SGR w.r.t. the incident angle. Uncertified 1445 reflectors are represented by blue squares, certified 1445.SN reflectors by red circles, and uncertified 1448 reflectors by green stars. The blue, red and green lines indicate corresponding fitted curves.

2.3 Radius and centring

One of the advantages of spherical reflectors lies in the combination of different types of instruments, such as levelling instruments, total stations, laser scanners, laser trackers, or photogrammetric cameras. The necessary conditions are an equality of the ball radii and an identical point of reference. For that purpose, points lying on the surface were observed by the AT960. Due to the glass-body and the drift-nest, parts of the surface were not accessible so that an enclosed configuration is not possible. The observations were performed in dynamic measurement mode, resulting in a point cloud of about 700 surface points for each SGR under investigation. Based on surface points and in accordance with ISO 10360-6 (2001), the centre point $\mathbf{X}_0$ and radius r were derived using an orthogonal distance fit (LÖSLER & ESCHELBACH, 2020). The optimization problem to be solved reads

$$\min \mathbf{e}^{\mathrm{T}}\mathbf{e} \quad \text{s. t.} \quad r^2 = \|\mathbf{X}_i - \mathbf{e}_i - \mathbf{X}_0\|_2^2, \tag{6}$$

where the i-th surface point reads $\mathbf{X}_i$, and $\mathbf{e}_i$ is the corresponding residual vector. This constrained nonlinear optimization problem was numerically solved by a Sequential Quadratic Programming approach as discussed by LÖSLER (2020, 2025).

To verify the measurement procedure, a 1.5″ steel ball (Aimess) was measured fourteen times. This reference steel ball is certified as grade G10 according to ISO 3290-1 (2014). The estimated mean radius reads 19.054 mm ± 1 µm, and deviates by 4 µm from the nominal value, cf. Fig. 6. The estimated centre is confirmed by the directly measured position of the reference SMR. The difference between both positions is 4 µm ± 1 µm, see also Fig. 7. Thus, the configuration is suitable to obtain the parameters r and $\mathbf{X}_0$.

The measurement procedure performed for each SGM comprised measuring the surface points as well as the centre of the SGM. This procedure was repeated three times for each SGM. Figure 6 depicts the estimated radii. Whereas the radii of certified 1445.SN reflectors are always smaller than the nominal value, the radii of the uncertified 1445 reflectors are greater than the nominal value. Differences of about 50 µm can be found. The radii of the 1448 reflectors are close to the nominal value and almost identical to those of the reference steel ball. Moreover, the repeatability is slightly better for uncertified reflectors. The standard deviations of the uncertified reflectors are of the same order of magnitude as those of the reference steel ball. Contrary, the standard deviations of the certified reflectors are about ten times larger.

The manufacturer's certificate specifies the centring deviation as the difference between the directly measured centres of a reference SMR and the SGM being tested. The distance corresponds to the centring deviation if and only if the radii of both spheres are identical. According to Fig. 6, this condition is not fulfilled, and the certified centring deviation depends on the orientation and the mounting of the reflectors. The distance between the sphere centre and the directly measured SGR position represents the centring deviation as the difference between the optical and geometric centres. It characterizes how precisely the glass-body is centred in the steel ball. This quantity is important when, for instance, polar observations are combined with levelling data, or in reverse engineering, where the observed position is reduced by the ball radius to the tactile measured surface.

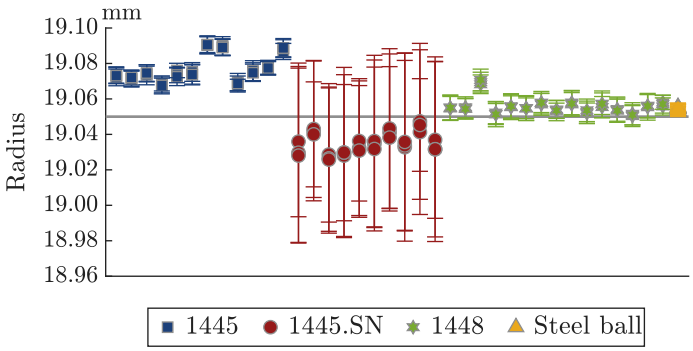

Fig. 6: Derived radii. Uncertified 1445 reflectors are represented by blue squares, certified 1445.SN reflectors by red circles, and uncertified 1448 reflectors by green stars. The results of the certified steel ball are shown in yellow. The solid line indicates the nominal value. Error bars (1σ) are scaled at a ratio of 20:1.

As shown in Fig. 7, the deviations are less than 250 µm. The repeatability is comparable for all lots under investigation. The standard deviations of the distances between the optical and the geometrical centres are 10 µm, and are dominated by the dispersion of the directly observed SGM position derived by uncertainty propagation.

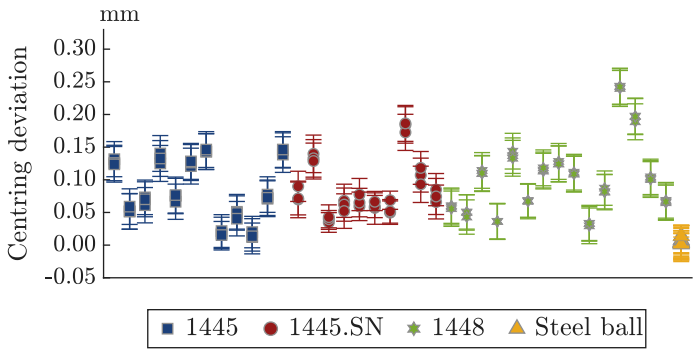

Fig. 7: Centring deviations of SGR, defined as the distance between the centre of the sphere and the directly measured SGR position, i.e., the optical and geometric centres. Uncertified 1445 reflectors are represented by blue squares, certified 1445.SN reflectors by red circles, and uncertified 1448 reflectors by green stars. For comparison, the difference between the reference SMR and the centre of the reference steel ball is shown in yellow. Error bars (1σ) are scaled at a ratio of 3:1.

In practical applications, where reflectors are exchanged or replaced by other spherical targets such as photogrammetric markers or scan targets, the centring and radius deviations overlap and must be taken into account. The combined deviation is cyclical and depends on the orientation and mounting of the reflectors. In the worst case, both deviations accumulate, resulting in a deviation greater than 200 µm.

2.4 Sphericity

The large standard deviations of the radii shown in Fig. 6 indicate greater surface roughness of the certified 1445.SN reflectors. According to ISO 1101 (2017), the sphericity describes the deviation from the spherical form. It is defined as the radial distance between two concentric spheres having an identical centre $\mathbf{X}_0$, i.e., the smallest circumscribed sphere with radius $r_{\min}$ and the greatest inscribed sphere with radius $r_{\max}$. Both spheres characterize the minimum zone $\Delta r = r_{\max} - r_{\min}$ containing all measured surface points. The corresponding optimization problem reads

$$\min\{r_{\max}^2 - r_{\min}^2\} \quad \text{s.t.} \quad \begin{aligned} 0 &\leq r_{\max}^2 - \|\mathbf{X}_i - \mathbf{X}_0\|_2^2 \\ 0 &\leq \|\mathbf{X}_i - \mathbf{X}_0\|_2^2 - r_{\min}^2 \end{aligned} \tag{7}$$

and is numerically solved by an interior point method. For a worthwhile contribution to the interior point method and practical algorithms, interested readers are referred to the textbook written by WRIGHT (1997).

In order to verify the sensitivity of the performed measurement procedure, fourteen repeated measurements of the certified steel ball were evaluated, because the sphericity of the ball is specified by 0.5 µm and provides a higher-order reference. The obtained minimum zone reads 10 µm $\pm$ 3 µm, which lies within the specification of the laser tracker, and confirmed the procedure.

Figure 8 depicts the derived minimum zone spheres and clearly confirms the assumption of greater surface roughness of the certified 1445.SN reflectors. The minimum zone spheres

within a lot are almost identical. The averaged minimum zone of the certified 1445.SN reflectors reads 135 µm ± 20 µm. The repeatability of the minimum zone spheres of the uncertified reflectors is noticeably higher. The mean values are 20 µm ± 3 µm and 30 µm ± 4 µm for the lots 1445 and 1448, respectively. Both values are close to the result obtained for the steel ball.

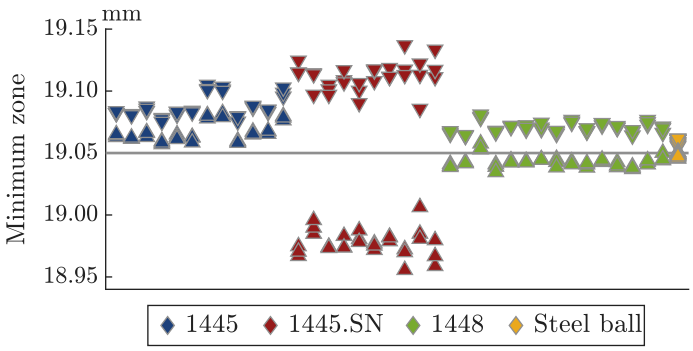

Fig. 8: Derived minimum zone spheres. The reflectors of the lots 1445, 1445.SN, and 1448 are coloured in blue, red, respectively, and green. Upward-pointing and downward-pointing triangles indicate the radii $r_{\min}$, $r_{\max}$, respectively. The results of the steel ball are shown in yellow. The solid line indicates the nominal value.

There is a significant difference in manufacturing quality between the ball housing of the reflectors used in different lots. The roughness of the surface affects the three-point support of the reflectors mounted in a drift-nest. Even if the glass-body is perfectly centred, unpredictable deviations occur when the alignment of the reflector changes.

3 Conclusion

Spherical glass-body reflectors and related accessories are becoming increasingly important in metrology and surveying engineering. The spherical design allows for a flexible combination of almost all relevant surveying techniques. The manufacturing precision of accessories has a significant impact on the uncertainty budgeting of the measurement process. In this contribution, thirty-six 1.5″ spherical glass-body reflectors of different lots manufactured between 2013 and 2025 were studied. Beside optical related quantities like the zero-point offset and misalignment effects, the dimension and the tolerance of form were examined in detail for the first time. A direct comparison of the lots revealed significant differences in both optical and geometrical properties. In the worst case, when the absolute values of the detected deviations are accumulated, the resulting error exceeds 0.5 mm. Thus, mixing reflectors from different lots should be avoided.

A high degree of repeatability of the measured quantities for reflectors from the same lot was observed. These reflectors are suitable for most terrestrial applications. However, it is recommended to validate the nominal values w.r.t. the instrument's wavelength and the field of application. For high-precision industrial applications, the reflectors should only be used in fixed installations and in configurations with restricted angles of incidence. The newly released 1448 reflector series exhibit manufacturing improvements. Ball radius, sphericity, and zero-

point offset are close to their nominal values. The remaining deviations are negligible for most total station applications.

Currently, there is no specific standard for reflectors that defines geometric properties and specifies quality standards. The establishment of such a standard would provide a basis for objective comparisons and is recommended by the authors.

Acknowledgments

We thank Thore Oliver Overath from Overath & Sand Vermessungsingenieure for providing the lot of the newly released 1448 reflectors. We also express our gratitude to the team of Bohnenstingl GmbH, in particular Klaus and Tim Bohnenstingl as well as Oliver Lang, for their support and fruitful discussions.

References

BAUER, P. & LIENHART, W. (2023). Augmentation approaches for geodetic permanent monitoring systems in dynamic urban environments. Surv Rev, 56(398), pp. 500–508. 10.1080/00396265.2023.2293555

BOHNENSTINGL GMBH (2022). Bohnenstingl – Surveying Tools and Accessories – Complete Catalog 2023, Version 221016.

BOHNENSTINGL GMBH (2025). Bohnenstingl – Surveying Tools and Accessories – Complete Catalog 2026, Version 251002.

FAVRE, C. & HENNES, M. (2000). Zum Einfluss der geometrischen Ausrichtung von 360°-Reflektoren bei Messungen mit automatischer Zielerfassung. VPK, 98(2), pp. 72–78. 10.5445/IR/1000010475

GUILLORY, J., TRUONG, D., WALLERAND, J.-P., & ALEXANDRE, C. (2024). A sub-millimetre two-wavelength EDM that compensates the air refractive index: uncertainty and measurements up to 5 km. Meas Sci Technol, 35(2), 025024. 10.1088/1361-6501/ad0a22

ISO 10360-6 (2001). Geometrical Product Specifications (GPS) – Acceptance and reverification tests for coordinate measuring machines (CMM) – Part 6: Estimation of errors in computing Gaussian associated features.

ISO 1101 (2017). Geometrical product specifications (GPS) – Geometrical tolerancing – Tolerances of form, orientation, location and run-out.

ISO 3290-1 (2014). Rolling bearings – Balls – Part 1: Steel balls.

KOPITZKE, K.-L. (2026). Prozessbegleitende Referenzlängenbestimmung von großen drehbaren Objekten in photogrammetrischen Anwendungen, VDVmagazin.

LACKNER, S. & LIENHART, W. (2016). Impact of Prism Type and Prism Orientation on the Accuracy of Automated Total Station Measurements. 3rd Joint International Symposium on Deformation Monitoring (JISDM).

LÖSLER, M. (2020). Zur Parameterschätzung mit unterschiedlichen Koordinatendarstellungen. zfv, 145(6), pp. 385–392. 10.12902/zfv-0319-2020

LÖSLER, M. & ESCHELBACH, C. (2020). Orthogonale Regression – Realität oder Isotropie? tm, 87(10), pp. 637–646. 10.1515/teme-2020-0063

LÖSLER, M., HAAS, R., & ESCHELBACH, C. (2013). Automated and continual determination of radio telescope reference points with sub-mm accuracy: results from a campaign at the Onsala Space Observatory. J Geod, 87(8), pp. 791–804. 10.1007/s00190-013-0647-y

LÖSLER, M. (2025). Zur Einordung der geodätischen Ausgleichungsrechnung in der numerischen Optimierung. zfv, 150(4), pp. 262–270. 10.12902/zfv-0508-2025

PAULI, W. (1969). Vorteile eines kippbaren Reflektors bei der elektrooptischen Streckenmessung. Vermessungstechnik, 17(11), pp. 412–415.

POLYANSKIY, M.N. (2024). Refractiveindex.info database of optical constants. Scientific Data, 11(1). 10.1038/s41597-023-02898-2

RÜEGER, J.M. (1978). Misalignment of EDM reflectors and its effects. Aust Surv, 29(1), pp. 28–36. 10.1080/00050326.1978.10441465

RÜEGER, J.M. (1996). Electronic Distance Measurement: An Introduction, 4 ed., Springer, Berlin. 10.1007/978-3-642-80233-1

VON SELLMEIER, W. (1871). Zur Erklärung der abnormen Farbenfolge im Spectrum einiger Substanzen. Annalen der Physik, 219(6), pp. 272–282. 10.1002/andp.18712190612

WIESER, A. (2026). Korrektur von Prismeneffekten auf Totalstationsmessungen. In Lienhart, W. (Ed.): Ingenieurvermessung 2026, Verlag der Technischen Universität Graz.

WRIGHT, S.J. (1997). Primal-Dual Interior-Point Methods. Society for Industrial and Applied Mathematics (SIAM), Philadelphia. 10.1137/1.9781611971453

XIA, Z., LUO, Y., ZHENG, Y., & PAN, H. (2006). Error analysis of a reflector in total station angle measurement. Third International Symposium on Precision Mechanical Measurements, Vol. 6280, 62802X. 10.1117/12.716307